

Influence of morphology on adsorbate-induced changes in thin-film dynamic conductivityG. Fahsold,¹ M. Sinther,² A. Priebe,¹ S. Diez,¹ and A. Pucci¹¹*Kirchhoff-Institut für Physik, Ruprecht-Karls-Universität Heidelberg, Germany*²*Institut für Angewandte Physik, Technische Universität Darmstadt, Germany*

(Received 13 April 2004; published 9 September 2004)

For ultrathin copper films of various morphology we studied adsorbate-induced changes in broadband infrared transmission at normal incidence of light. Smooth Cu films on Si(111) and mesoscopically rough Cu films on KBr(001) were exposed to CO and to C₂H₄. We observed significant broadband changes for each of these gases and for both surfaces. Applying a Drude-type model we calculated the optical spectra in accord with the experiment. We find that the effects related to a change in the electronic relaxation rate are weakly influenced by the mesoscopic roughness of the film, while the effects related to charge transfer are strongly enhanced due to such roughness. This paper shows that the real adsorbate-induced changes can be determined for both the homogeneous films and the inhomogeneous films beyond percolation. The increased surface area owing to mesoscopic roughness is merely one contribution to larger adsorbate-induced effects of inhomogeneous films. The other more interesting contribution is due to depolarization in rough metal films that is responsible for strong enhancement of charge transfer effects.

DOI: 10.1103/PhysRevB.70.115406

PACS number(s): 78.20.-e, 68.43.-h, 78.30.-j, 73.25.+i

I. INTRODUCTION

The elastic mean free path of electrons in bulk metals, e.g., Cu at room temperature, is up to several ten nanometers. As a consequence, if current is carried by metal nanostructures with a size in the few 10 nanometer range, the resistance is already strongly influenced by the structural and chemical nature of the nanostructure interfaces with the environment. This so-called surface or adsorbate-induced resistivity is of fundamental importance for an understanding of nanostructure electronic properties and for the development of nanostructure based applications. Adsorbate-induced resistivity of thin films has been demonstrated in dc resistivity measurements,¹⁻⁴ infrared (ir) broadband reflectivity experiments,^{1,2} and by optical spectroscopy.^{5,6} Surface-enhanced ir-absorption (SEIRA) may also be influenced by the scattering between adsorbates and conduction electrons, which has been demonstrated in a very recent study on the origin of the Fano-type line shape of surface-enhanced ir absorption by adsorbate vibrations.^{7,8}

An early study of the morphology dependence of adsorbate-induced surface resistivity was done by Wißmann via dc-resistivity experiments.³ For films of various morphology he found roughly the same increase of resistivity per adsorbate molecule at the beginning of exposure. However, smooth films showed a smaller maximum change when compared with rough films. Later, he also addressed the influence of thin film morphology on the adsorbate-induced change in ellipsometry data.⁶ Again, annealed films showed smaller effects compared to granular films. However, due to a lack of detailed information on surface roughness, an analysis of the quantitative relations between surface roughness and adsorbate effects was not possible.

Classically, in a certain vicinity to the surface adsorbates can induce a change $\Delta\omega_\tau$ in the relaxation rate ω_τ of free charge carriers and a change Δn in their density n .^{1,3} For a thin film of thickness d and a mean free path l_{MFP} of the free charge carriers, both effects lead to a change $\Delta\rho$ in the resistivity ρ , i.e.,

$$\Delta\rho = \rho \cdot \frac{l_{\text{MFP}}}{d} \cdot \left(\frac{\Delta\omega_\tau}{\omega_\tau} - \frac{\Delta n}{n} \right) = \rho \cdot \frac{l_{\text{MFP}}}{d} \cdot \frac{\Delta\omega_\tau}{\omega_\tau} \cdot C^*, \quad (1)$$

with

$$C^* = 1 + \frac{-\Delta n/n}{\Delta\omega_\tau/\omega_\tau}. \quad (2)$$

For a broad number of adsorbate/thin-film systems, a negligibly small Δn can be assumed, as it is done for the scattering model of surface resistivity by Persson.⁹⁻¹¹ Then, $\Delta\rho$ is dominated by $\Delta\omega_\tau$ and $C^* = 1$. Tobin found that the surface resistivity model could be tested by comparing $\Delta\rho$ with adsorbate-induced changes in the reflectivity of metal surfaces for p -polarized infrared light.¹ Such changes ΔR_p have been extensively studied within the recent years.^{1,2,12-17} They were predicted to be proportional to $\Delta\rho$ (measured for thin films),^{2,9-11} i.e.,

$$\frac{\Delta R_p}{\Delta\rho} = -\frac{\omega_p^2 \epsilon_0}{c} \cdot \frac{4d \cos \theta}{\cos^2 \theta + \omega^2/\omega_p^2} \cdot \frac{1}{C^*}, \quad (3)$$

with ω_p being the bulk plasma frequency of the metal, c the speed of light, ϵ_0 the electric constant and θ the angle of incidence with respect to the surface normal. For $C^* = 1$ the ratio $\Delta R_p/\Delta\rho$ should neither depend on the kind of adsorbate and the adsorbate coverage, nor on morphology-dependent scattering rates.

Tobin experimentally investigated the factor C^* for pure copper films¹⁸ and found that it varied with the type of adsorbate, which means that Δn cannot be neglected.¹ But, surprisingly C^* also varied with the morphology of the films (see Table 1 in Ref. 1 and Fig. 8 in Ref. 1). For films with the lower conductivities, i.e., higher ω_τ [as-grown films on Si(100) (Refs. 13 and 19)], he found higher C^* values compared to films with the higher conductivities and lower ω_τ [annealed Cu films on glass¹² and on TiO₂(110)²]. Following Eq. (2), it seems that for the rough low-conductivity films the



FIG. 1. Sketch of the two types of Cu films that are investigated in this work: mesoscopically smooth films on Si and mesoscopically rough films on KBr. Due to the same growth temperature the same adsorption properties are expected for the surfaces of these films.

changes $\Delta n/n$ (with $\Delta n < 0$) are enhanced with respect to the changes $\Delta\omega_p/\omega_p$. Tobin calculated the corresponding charge transfer Δn and found unreasonably high values for it.¹ An even dominant role of $\Delta n/n_B$ must be concluded from experiments with formic acid exposure of rough copper films where a resistivity change but no reflectivity change was observed.^{1,19} According to Eqs. (2) and (3), this corresponds to $-\Delta n/n \gg \Delta\omega_p/\omega_p$. These results point to unexpectedly strong effects of charge transfer and cannot be explained without looking at the real film morphology.

Here, we present a study which explains how the changes of measured quantities due to adsorbate-induced charge carrier relaxation and adsorbate-induced charge transfer are modified by the mesoscopic roughness of a real film. We present broadband infrared spectroscopic results for adsorption of CO and of C_2H_4 on two types of continuous (conducting) copper films as shown in Fig. 1: mesoscopically smooth films grown on Si(111) and mesoscopically rough films grown on KBr(001). Despite the different mesoscopic roughness, which is due to the different surface diffusion properties for Cu atoms on the two substrates, a similar degree of atomic roughness can be expected for the surfaces owing to the growth at the same substrate temperature. We studied the morphologies by *in-situ* IR spectroscopy during film growth and by *ex-situ* atomic force microscopy (AFM) at the final film thickness. The measured adsorbate-induced changes in the broadband transmission (ACBT) for the two adsorbates and for the two morphologies were analyzed with respect to $\Delta\omega_p^2/\omega_p^2$ and $\Delta\omega_p/\omega_p$. The influence of a mesoscopic film roughness on these parameters is theoretically investigated on the basis of the two-dimensional (2D) Bruggemann model. These calculations let us conclude that the electric depolarization due to a rough film microstructure gives an enhanced sensitivity of the measured conductivity to adsorbate-induced charge transfer. This effect explains unreasonably high values for the adsorbate-induced changes of the electron density that have been reported in Ref. 1.

II. THEORETICAL BACKGROUND

In previous work^{20,21} we have shown that for homogeneous metal thin films (with average film thickness d) the ir-optical properties may be described with local optics on the basis of Drude-type dielectric function

$$\epsilon_{\text{film}}(\omega, d) = 1 - \frac{\omega_{p \text{ film}}(\omega, d)^2}{\omega \cdot [\omega + i\omega_{\tau \text{ film}}(\omega, d)]} \quad (4)$$

with ω the circular frequency.²² Note, for the calculation of spectra in the mid-ir and even for copper it is important to

take account of the frequency dependence of the Drude parameters $\omega_{p \text{ film}}$ and $\omega_{\tau \text{ film}}$.²⁰ The mid-ir frequency dependence is not due to contributions from interband transitions that are expected for higher photon energies, i.e., above ~ 1.5 eV for copper.^{23,24} For metal optics well below this threshold, we use the typical background $\epsilon_{\infty} = 1$.²⁵

For rough metal films one must consider that depolarization effects (stray fields) change the optical response to the external field compared to the response of a smooth film. Effective media theories have been developed for various geometries and dimensionalities.^{26–28} But beyond the percolation threshold, the ir-optical properties of rough metal films can also be described by a Drude-type dielectric function, as it has been shown in theory²⁹ and in experiment.²¹

Now we want to analyze this easy description of inhomogeneous but continuous metal films again, looking at the consequences for an interpretation of adsorbate effects in experimental studies of the conductivity. We start with the analytic approach to the dielectric function of inhomogeneous media that originally was developed by Bruggemann.²⁸ This theory holds particularly for thin films if the two components occur on a topological equivalent level.^{30,31} Even for films formed from arrays of regularly shaped islands⁷ we found from the IR analysis in the vicinity of the percolation threshold (above and below) that the Bruggemann theory (BT) is well suited for the calculation of thin film ir-optical properties.⁷ BT has been applied by Persson and Demuth³² to determine the frequency dependent resistivity of metal ultrathin films on silicon. Zhang and Stroud³³ showed that BT well describes the numeric simulations of the dynamic conductivity of inhomogeneous metal thin films. They also find that BT can easily be extended even to account for the dimensional crossover from two to three dimensions as the film thickness increases.

Let us calculate the dielectric function ϵ_B for a two-dimensional mixture of a metal (with volume fraction F) and a dielectric (with volume fraction $1-F$) according to BT by solving the equation

$$F \frac{\epsilon_m - \epsilon_B}{\epsilon_m + \epsilon_B} + (1-F) \frac{\epsilon_d - \epsilon_B}{\epsilon_d + \epsilon_B} = 0 \quad (5)$$

for ϵ_B . Here, the dielectric functions of the two components are ϵ_m for the metal, with

$$\epsilon_m(\omega) = 1 - \frac{\omega_{pm}^2}{\omega \cdot (\omega + i\omega_{\tau m})}, \quad (6)$$

and a constant ϵ_d for the nonmetal. This leads to

$$\epsilon_B = \epsilon_m \cdot \left[\left(1 - \frac{\epsilon_d}{\epsilon_m} \right) \left(F - \frac{1}{2} \right) \mp \sqrt{\left(1 - \frac{\epsilon_d}{\epsilon_m} \right)^2 \left(F - \frac{1}{2} \right)^2 + \frac{\epsilon_d}{\epsilon_m}} \right], \quad (7)$$

where the sign of the square root must be chosen to fulfill $\text{Im } \epsilon_B \geq 0$. Except for F in the vicinity of the critical filling F_c , which is $1/2$ in two dimensions,³⁴ the negative sign of the root is valid. In this work we only consider $F > F_c$, i.e.,

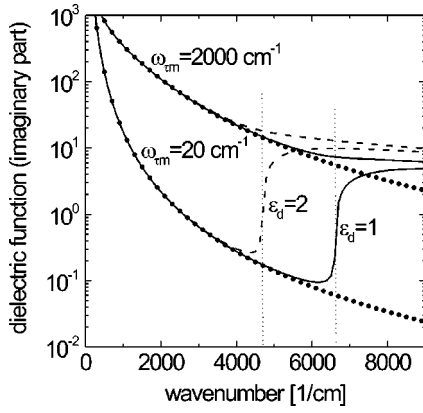


FIG. 2. Imaginary part of the dielectric function ϵ_B for a two-dimensional inhomogeneous medium composed of 60% ($F=0.6$) copper ($\omega_{Pm}=66\,000\text{ cm}^{-1}$) and 40% dielectric with $\epsilon_d=1$ (solid lines) and with $\epsilon_d=2$ (dashed lines). The values for the relaxation ω_m are 20 cm^{-1} (lower curves) and 2000 cm^{-1} (upper curves). Below the high wave number limit ω_{\max} (vertical lines for the two values of ϵ_d) the effective medium is well described by a Drude-type dielectric function $F \cdot \epsilon_{D\text{ eff}}$ (circles) with $\omega_{P\text{ eff}}^2=0.335 \cdot \omega_{Pm}^2$ and $\omega_{\tau\text{ eff}}=\omega_m$.

conducting films with a volume filling beyond the percolation threshold.

For copper films with $\omega_{Pm}=66\,000\text{ cm}^{-1}$ (Ref. 25) and $F=0.6$ the imaginary part of ϵ_B from Eq. (7) is shown in Fig. 2. The relaxation of the metal component has been chosen to be roughly corresponding to either bulk properties ($\omega_m=20\text{ cm}^{-1}$) or thin film properties [typically $\omega_m=2000\text{ cm}^{-1}$ (Ref. 20)]. For simplicity, the frequency dependencies of the Drude parameters are ignored in this calculation. The dependence of $\text{Im } \epsilon_B$ on ϵ_d is demonstrated with the curves for $\epsilon_d=1$ and $\epsilon_d=2$. $\epsilon_d > 1$ would be relevant for films with adsorbate multilayers for example. The frequency dependence of $\text{Im } \epsilon_B$ seems to divide into two regimes: a low-frequency regime, where $\text{Im } \epsilon_B$ is almost independent from ϵ_d , and a high-frequency regime, where $\text{Im } \epsilon_B$ is dominated by ϵ_d . This division is the more pronounced the smaller the relaxation. It is obvious that the transition between the two regimes strongly depends on ϵ_d . As we want to investigate conducting films beyond the percolation threshold, the metal-like effective properties in the low frequency regime and its upper frequency limit are of interest for this paper.

For a calculation of the mid-ir absorption of a real film with ϵ_B we use an effective Drude-type dielectric function and the average thickness d which is related to the amount of metal per unit area. If d is in the nanometer range it can be assumed that

$$d \cdot \text{Im } \epsilon_{D\text{ eff}} = d_{\text{opt}} \cdot \text{Im } \epsilon_B \quad (8)$$

with $d_{\text{opt}}=d/F$ as the optical thickness of the Bruggemann effective medium. The effective quantity $\epsilon_{D\text{ eff}}(\omega)$ corresponds to $\epsilon_m(\omega)$ of Eq. (6) with the only difference that ω_{Pm} and ω_m are substituted by effective parameters $\omega_{P\text{ eff}}$ and $\omega_{\tau\text{ eff}}$. We find that Eq. (8) is reasonable if

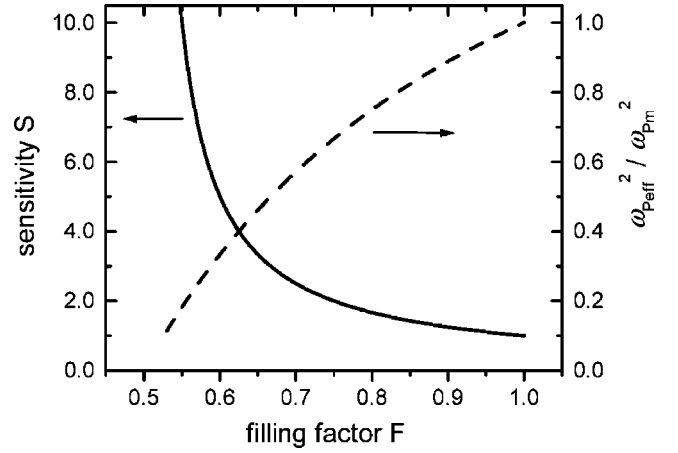


FIG. 3. Dependence of $\omega_{P\text{ eff}}^2/\omega_{Pm}^2$ and the relative sensitivity $S=(\partial\omega_{P\text{ eff}}^2/\partial F)/(\omega_{P\text{ eff}}^2/F)$ on the metal filling factor F for two-dimensional films.

$$\left| \frac{\text{Re } \epsilon_m}{\epsilon_d} \right| \gg \frac{1}{(F - F_c)^2} - 2 \quad (9)$$

is fulfilled. Vice versa, a film with F fulfilling this relation may be described by a Drude-type dielectric function (see the dotted lines in Fig. 2). For ω and ω_m both in the mid-ir, or below, relation (9) corresponds to a spectral range $\omega < \omega_{\max}$, where to a good approximation

$$\omega_{\max} = \omega_{Pm} \cdot (F - F_c)/\sqrt{\epsilon_d}. \quad (10)$$

There is no significant dependence of ω_{\max} on the relaxation ω_m . A small change of ϵ_d , e.g., due to gas adsorption in the voids, modifies ω_{\max} but it does not influence $\omega_{P\text{ eff}}$ and $\omega_{\tau\text{ eff}}$ in the spectral range $\omega < \omega_{\max}$ (see Fig. 2). On the other hand, for $\omega > \omega_{\max}$ or for F near F_c and ω in the ir, changes in ϵ_d lead to significant contributions to the ACBT.⁷

Equation (8) gives a plasma frequency $\omega_{P\text{ eff}} < \omega_{Pm}$. This can easily be seen in the limit $\omega \ll \omega_{\max}$, where Eq. (5) reduces to

$$\epsilon_B = (2F - 1) \cdot \epsilon_m. \quad (11)$$

According to Eq. (8), this equality gives $\omega_{P\text{ eff}}^2/\omega_{Pm}^2$ as

$$\omega_{P\text{ eff}}^2/\omega_{Pm}^2 = 2 - 1/F. \quad (12)$$

This dependence is shown in Fig. 3. The effective plasma frequency $\omega_{P\text{ eff}}$ decreases with decreasing metal filling and it approaches zero values in the vicinity of the percolation threshold at $F=F_c=0.5$. We want to emphasize that the physical origin of the relation $\omega_{P\text{ eff}} < \omega_{Pm}$ is not the reduced charge density in the metal-dielectric mixture, as this reduction is already compensated by weighting $\text{Im } \epsilon_B$ with the factor F^{-1} [see Eq. (8)]. Instead, its reason is the insertion of empty volume which causes depolarization.

Before we show that Eq. (12) has a severe consequence for the optical measurement of the charge transfer involved with adsorption, we want to remind that charge transfer at surfaces is treated in two different ways in the literature. In local optics applied to surfaces, the surface position is usually kept constant and only the optical properties in the sur-

face region (which is the whole thin film in our case) are allowed to change. Correspondingly, the charge transfer (e.g., involved with a chemical reaction at a surface) is described by a small change Δn . In a more atomistic picture such charge transfer is described with n unchanged but with a change in the total number of metal atoms. While for a smooth film ($F=1$) this can be expressed by a change Δd of film thickness d , for a rough film ($F < 1$) a change ΔF of the filling factor F might be more descriptive. The equivalence of these pictures is expressed by the relation

$$\Delta d = \frac{\Delta n}{n} \cdot d = \frac{\Delta F}{F} \cdot d. \quad (13)$$

In the following we will use Δd as a measure of the transferred amount of charge.

The effect of charge transfer on the dielectric-function parameter $\omega_{P \text{ eff}}$ follows from Eq. (12). If we define an *effective* charge transfer

$$(\Delta d)_{\text{eff}} = \frac{\Delta \omega_{P \text{ eff}}^2}{\omega_{P \text{ eff}}^2} \cdot d, \quad (14)$$

we find that it is related to the true charge transfer by

$$(\Delta d)_{\text{eff}} = S \cdot \Delta d \quad (15)$$

with

$$S = \frac{1}{2F - 1}. \quad (16)$$

The parameter S can be interpreted as an enhancement factor that accounts for the increased optical sensitivity to Δd . For a film with F in the interval $F_c < F \leq 1$, the value for $(\Delta d)_{\text{eff}}$ from a Drude-type analysis of experimental (e.g., optical) data overestimates the true charge transfer Δd . The degree of overestimation increases with decreasing F as shown in Fig. 3. For example, for $F=0.55$, the overestimation is by an order of magnitude.

Now, let us consider the adsorbate-induced change $\Delta \omega_{\tau m}$ in the relaxation of charge carriers. From Eq. (8) and (11) it comes out that

$$\omega_{\tau \text{ eff}} = \omega_{\tau m}. \quad (17)$$

This equality means that the real adsorbate-induced change in the relaxation is directly obtained from a Drude-type analysis of spectra. For both the adsorbate-induced changes ΔF and $\Delta \omega_{\tau m}$ it is important to note that simply because the larger surface of an inhomogeneous film accepts more adsorbates the changes can be increased with respect to smooth films.

Before we report on our experiments and the ir-spectroscopic results we want to shortly describe their analysis performed on the basis of the Drude-type model [see Eq. (4)].^{20,21} The application of this model is reasonable as for more advanced models the number of unknown parameters is rather large. In reality, detailed knowledge on the morphology, the dimensionality, and the filling factor F of the metal films is absent in most cases. Furthermore, the value for ϵ_d is unclear for a thin film between two different dielectrics

(vacuum and the thin film substrate). Additionally, in a medium which is inhomogeneous on a nanoscale the Drude parameters of the metal component are unknown because of classical and quantum mechanical size effects. The Drude-type analysis of spectra of such inhomogeneous metal films allows to keep the number of free parameters low with the only restriction that the frequency range is limited by $\omega < \omega_{\text{max}}$ [or for a given frequency range by $F > F_{\text{min}}$, with F_{min} from Eq. (9)]. Then, as we calculate the thickness d of a film from deposition parameters, only two fit parameters are left. Since we use the convenient thin-film formulation with

$$\omega_{P \text{ film}}(\omega, d) = \beta(d) \cdot \omega_{P \text{ bulk}}(\omega) \quad (18)$$

and with

$$\omega_{\tau \text{ film}}(\omega, d) = \omega_{\tau 0}(d) + 9.57 \times 10^{-2} \cdot \omega \quad (19)$$

for copper at 100 K, our fit parameters are $\beta(d)$ and $\omega_{\tau 0}(d)$. The frequency independent factor $\beta(d)$ accounts for depolarization effects and possible size effects,^{20,21,35} while the frequency dependent bulk plasma frequency $\omega_{P \text{ bulk}}(\omega)$ is calculated from tabulated data.²⁵ The relaxation $\omega_{\tau}(\omega, d)$ accounts for the frequency dependence of the bulk relaxation rate in copper²⁰ and it allows a thickness dependent adjustment of the total relaxation to include scattering from defects and thin film interfaces. For calculating ir spectra we use commercial software³⁶ which allows a fully coherent treatment of field amplitudes.

As the spectra of the ACBT are normalized to those of the unexposed films, we start the spectral fits with the parameters β^2 and $\omega_{\tau 0}$ derived from the clean, unexposed film's ir spectrum and vary them to get values for the exposed films. The corresponding changes are $\Delta \omega_{P \text{ film}}^2 = \omega_{P \text{ film-exposed}}^2 - \omega_{P \text{ film-unexposed}}^2$ and $\Delta \omega_{\tau 0} = \omega_{\tau 0 \text{ exposed}} - \omega_{\tau 0 \text{ unexposed}}$. Adsorbate-induced changes in the frequency dependence of $\omega_{P \text{ film}}$ and $\omega_{\tau 0}$ are neglected in this study. Further details of our calculations have been given in Ref. 20.

III. EXPERIMENT

Our experimental setup consists of a Fourier transform ir spectrometer (BRUKER IFS66v/S) and a mercury cadmium telluride (MCT) detector which are connected to an ultrahigh-vacuum (UHV) preparation chamber with base pressure below 2×10^{-8} Pa. A low-energy electron diffraction (LEED) system allows *in-situ* characterization of the crystalline quality of prepared surfaces.

Aiming at surfaces of different mesoscopic roughness (see Fig. 1) we prepared Cu films on silicon and on KBr. KBr(001) surfaces were prepared by cleavage in air followed by a degassing in UHV at 473 K for a period of 3–4 h. For Si(111), we used high resistivity ($>8000 \Omega \text{ cm}$) hydrogen terminated *n*-type silicon³⁷ and thermally processed it under UHV. The Si surfaces that gave smooth Cu films we call Si[I] and Si[II]. The thermal processing for Si[I] was heating to 1270 K for ~ 1 min. This leads to a 7×7 surface reconstruction which was checked with LEED. The Si[II] sample was heated to only 1130 K for ~ 1 min. At this temperature the hydrogen is desorbed but the phase transition to the

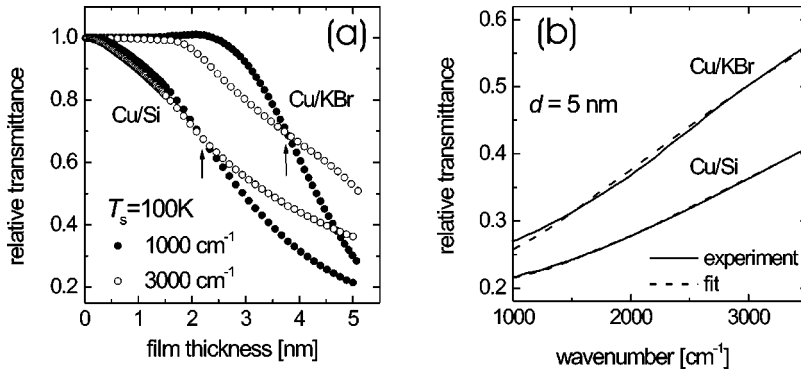


FIG. 4. The relative transmittance $T_{\text{film}}/T_{\text{substrate}}$ of copper films on KBr and on Si[II] at $T_s=100$ K normalized to the transmittance of the bare substrate is shown (a) versus film thickness for two different wave numbers and (b) versus wave number for a thickness $d=5$ nm. The arrows in (a) indicate an optical crossover for the selected wave numbers at a thickness d_c . They roughly mark the onset of metallic conductivity. In (b) also the spectral fits to the experimental data are shown.

7×7 superstructure is not yet entirely proceeded.³⁸

An electron impact evaporator (OMICRON EFM3) was used for Cu deposition on the substrates. For all films the average film thickness d was calculated from the deposition time and the deposition rate (typically 0.1 nm/min) which was calibrated for each experiment with a quartz microbalance. The Si and KBr substrate temperature T_s during metal deposition was 100 K. Only for the 7 nm film on Si[I] T_s was raised to 400 K during an intervening period of Cu deposition (for $4 \text{ nm} < d < 5 \text{ nm}$). At 400 K surface diffusion is already fast but silicide formation has not yet started.³⁹ Each film preparation was monitored by recording ir transmittance spectra at normal incidence of light. For one spectrum (800 cm^{-1} to 4200 cm^{-1} , resolution 32 cm^{-1}) 100 scans were sampled within 7 s.

At the final thickness and still at $T_s=100$ K the films were exposed to either CO (purity 99.997 vol %) or C_2H_4 (purity 99.95 vol %) at a partial pressure of typically 2×10^{-6} Pa (ion-gauge readout). During exposure we measured the ACBT with a spectral resolution of 4 cm^{-1} (100 scans per spectrum sampled in 20 s) and in steps of ~ 0.3 L (1 L = 1.33×10^{-4} Pa s). Figure 2 in Ref. 20 demonstrates the typical course of the experiments.

For further characterization of the morphologies of the films *ex-situ* AFM measurements were performed quickly after transferring the samples to air. On various locations on the samples imaging was done in tapping mode with a Digital Instruments Nanoscope III using tips with a radius of 5–10 nm.

TABLE I. Parameters used for calculating the transmittance of copper thin films and the adsorbate-induced change in the broadband transmission (ACBT) for exposures above saturation to several adsorbates at 100 K: film thickness d , thickness d_c of optical crossover, depolarization $\beta^2 = \omega_p^2 \text{ film} / \omega_p^2 \text{ bulk}$ and zero-frequency relaxation rate $\omega_{\tau 0}$. The change in surface resistivity is given as $d \cdot \Delta \omega_{\tau 0} = d \cdot (\omega_{\tau 0} \text{ exposed} - \omega_{\tau 0} \text{ unexposed})$ and for the effective charge transfer the value of $(\Delta d)_{\text{eff}} = d \cdot (\omega_p^2 \text{ film-exposed} / \omega_p^2 \text{ film-unexposed} - 1)$ is shown. Assuming $\omega_p^2 \text{ film} / \omega_p^2 \text{ bulk} = 2F - 1$ we calculated the sensitivity S and the true charge transfer Δd (see text). The films were grown and exposed to the adsorbates at ~ 100 K.

Film	Substrate	Before exposure				Adsorbate	Exposure (L)	Changes after exposure			
		d (nm)	d_c (nm)	$\omega_p^2 \text{ film} / \omega_p^2 \text{ bulk}$	$\omega_{\tau 0}$ (cm^{-1})			$d\Delta\omega_{\tau 0}$ ($\text{cm}^{-1} \text{ nm}$)	$(\Delta d)_{\text{eff}}$ (nm)	S	Δd (nm)
		± 0.2	± 0.1	± 0.01	± 40		± 0.5	± 25	± 0.01	± 0.2	± 0.01
Cu	Si(111) [I]	7.0	2.1	1.06	3102	CO	5.0	833	0.03	0.9	0.03
Cu	KBr(001)	5.1	3.7	0.36	1514	CO	8.8	1051	0.08	4.5	0.02
Cu	Si(111) [II]	5.0	2.2	0.93	2097	C_2H_4	17.5	305	0.02	1.1	0.02
Cu	KBr(001)	5.7	3.7	0.32	2071	C_2H_4	17.8	660	0.14	5.3	0.03

IV. RESULTS AND DISCUSSION

A. Thin film growth and morphology

The spectra measured during Cu deposition on KBr and on Si indicate that with increasing average film thickness d the relative ir transmission $T_{\text{film}}/T_{\text{substrate}}$ decreases. This decrease is found for the whole spectral range and it is shown in Fig. 4(a) for two representative wave numbers (in the case of Cu/KBr a very weak increase of ir transmittance at 2–2.5 nm film thickness is found due to a reduction of substrate reflectivity by a Cu $3d$ -island film). In the beginning of metal deposition $T_{\text{film}}/T_{\text{substrate}}$ is lower for the higher frequency. Around a certain thickness this situation reverses, i.e., $T_{\text{film}}/T_{\text{substrate}}$ is almost independent from frequency there. The thickness d_c for this optical crossover is between 2 nm and 4 nm (see Table I). Even though for all samples the spectra at 5 nm thickness exhibit a metal-like dispersion $\partial(T_{\text{film}}/T_{\text{substrate}})/\partial\omega > 0$ [Fig. 4(b)], the almost two times larger d_c for Cu/KBr and the higher transmission of these samples already suggest a more rough mesoscopic morphology for Cu/KBr and a more smooth morphology for Cu/Si.

Before performing a Drude-type analysis of such spectra, we should check the volume filling F of the films with respect to ω_{max} of Eq. (10) and relation (9). For copper, since the frequency dependence of $\omega_p \text{ bulk}$ is weak, we can take d_c as the critical thickness for percolation.^{21,40,41} For all films of this ACBT study, the final thickness d is more than 30% above d_c . For estimating the corresponding volume filling F

we consider 3d-island growth modes where the island height does not increase faster than the island diameter. Then we get $\partial F/\partial d \geq (2/3)(F/d)$ for a film where island nucleation has finished and coalescence has not yet started. Assuming this relation even in the vicinity of the percolation transition, we find that $F \geq F_c \cdot (d/d_c)^{2/3}$ and that the films at the final thickness should have a volume filling of more than 20% above F_c . We note that this is a rough estimation as elastic strain and surface diffusion barriers can lead to a columnarlike growth⁷ and therefore slow down the filling of the film volume with deposited material. Nevertheless, using $F \geq 0.6$ for a calculation of the spectral range for a Drude-type description of ir spectra, we find $\omega_{\max} \geq 0.1 \cdot \omega_{P \text{ bulk}}$ for the films in vacuum, which is above the spectral range in our experiments.

As demonstrated in Fig. 4, we succeed in describing the thin-film ir spectra by only varying the two parameters $\omega_{P \text{ film}}$ [i.e., β , see Eq. (18)] and $\omega_{\tau 0}$ [see Eq. (19)]. The found best-fit values for these parameters are given in Table I.

While $\omega_{P \text{ film}}$ is around $\omega_{P \text{ bulk}}$ for Cu/Si, it is far below $\omega_{P \text{ bulk}}$ for Cu/KBr. For the films on Si[I] and on Si[II] this indicates absence of depolarization effects and therefore a smooth morphology. The slightly larger $\omega_{P \text{ film}}$ for the Si[II] substrate is possibly due to the temperature variation during Cu deposition (see Sec. III). The small $\omega_{P \text{ film}}$ values for the films on KBr are a clear indication for depolarization owing to a granular morphology of these films.^{21,35} Assuming $\omega_{P \text{ film}}^2/\omega_{P \text{ bulk}}^2 \approx 2 - 1/F$ according to Eq. (12), i.e., neglecting quantum size effects of $\omega_{P \text{ film}}^2$, we get $F \approx 1$ for Cu/Si and $F \approx 0.6$ for Cu/KBr. Note that these values are consistent with our above estimation of filling factors from d_c values.

Concerning charge carrier relaxation, the value of $\omega_{\tau 0}$ is roughly 1000 to 3000 cm^{-1} for all films (see Table I) which is more than a factor of 10 stronger than the relaxation of bulk Cu at 100 K [$\omega_{\tau 0} = 45 \text{ cm}^{-1}$ (Ref. 42)]. This cannot be explained by only the classical size effect for a single-crystalline homogeneous film with zero specularity,⁴³ as $l_{\text{MFP}}/d \approx 7$ in our case at mid-ir frequencies.⁴⁴ As we know from our Fe-thin-film studies,^{21,44} the relaxation is strongly enhanced in inhomogeneous thin films. Because of the small $\omega_{P \text{ film}}^2/\omega_{P \text{ bulk}}^2$ values for Cu/KBr, we propose the mesoscopic roughness of the film as the main origin of the large $\omega_{\tau 0}$ values for Cu/KBr. However, for Cu/Si we have determined similar or even larger values for $\omega_{\tau 0}$, even though $\omega_{P \text{ film}}^2/\omega_{P \text{ bulk}}^2 \approx 1$ for these films. Since we suppose from AFM and from ir spectra after CO exposure (see below) that these films do not have a significant mesoscopic roughness, our explanation for the large $\omega_{\tau 0}$ values are structural defects inside the films (e.g., grain boundaries) and chemical disorder at the interface to silicon. From the smaller d_c values (compared to Cu/KBr) and from the fact that we could observe only a faint ringlike diffraction structure by LEED we conclude a polycrystallinity with rotational domains and grain sizes significantly smaller than in the case of Cu/KBr. Grain boundary scattering can effectively increase the dc resistivity of Cu films on Si (Ref. 45) and of Cu nanowires.⁴⁶ Chemical disorder is concluded from the literature, where

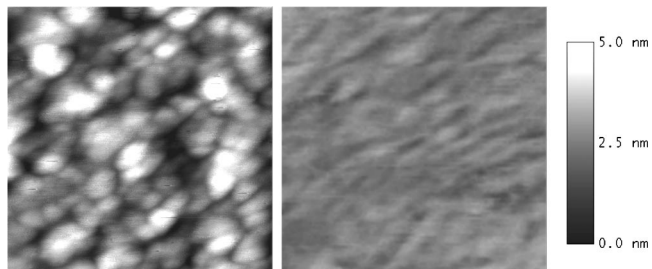


FIG. 5. AFM images of mesoscopically rough Cu films on KBr(001) (left) and of smooth Cu films on Si(111)[II] (right). Film thickness is 5.5 nm for both films. Imaging is done in air at room temperature, scan size is $200 \text{ nm} \times 200 \text{ nm}$. Both films are grown at 100 K.

irregular RHEED (reflecting high-energy electron diffraction) oscillations are reported for the first nanometer of Cu on Si(111) 7×7 at $\sim 120 \text{ K}$ which is interpreted as silicide formation and interdiffusion at the interface.^{47,48} The stronger relaxation for Cu/Si[I] (compared to Cu/Si[II]) is probably due to stronger intermixing as a result of the temporarily higher temperature during deposition (see Sec. III). From annealing experiments and dc-resistivity measurements we know that for 5 nm Cu/Si(111) (grown and investigated at 100 K) ω_{τ} is strongly increased after heating to 400 K. This increase is not due to a change of the surface shape, as $\omega_{P \text{ film}}^2/\omega_{P \text{ bulk}}^2$ is observed to remain almost unchanged.

Information on mesoscopic roughness can also be obtained from ir spectra after adsorbate exposure.⁷ For Cu/KBr we observe strong adsorbate vibrational structures (due to SEIRA) after exposure to CO or to C_2H_4 (see Fig. 6, and Sec. IV B for details). The occurrence of SEIRA at normal incidence of light and its strength is a consequence of metal film roughness.^{7,41,49} For Cu/Si no SEIRA is observed.

The results of our characterization of Cu films on KBr and on Si[II] by AFM are shown in Fig. 5. Both images were taken *ex-situ* at room temperature about 1 hour after the samples were transferred to air. From thermal desorption experiments and ir-spectral measurements after *in-situ* heating of the films to $\sim 300 \text{ K}$ we know that the ir transmission decreases due to an annealing of the films but the morphology dependent SEIRA effects indicate only minor changes in the morphology. The spectral changes correspond to a smoothing of atomic roughness and not to a change of mesoscopic shape. We can also exclude strong effects due to exposure to air. With increasing exposure of 5.5 nm Cu on KBr (grown at 100 K) we find an increase of ir transmission, but after 15 hours in air the ir transmission still indicates metallic conductivity, i.e., the films remain beyond the percolation threshold. As the films on the two different substrates (KBr and Si) were handled the same way and as Cu shows only moderate reactivity to ambient air, the significant differences in mesoscopic surface shape should still be present during imaging.

The Cu films on KBr are mesoscopically rough with well-defined grains of typically 20 nm size (from center to center) and typically 3 nm height (from top to valley). The lateral size of the grains is only little below l_{MFP} , which is 34 nm for bulk Cu at 100 K and at $\omega = 2000 \text{ cm}^{-1}$ [see Eq. (19)]. The

pronounced edges of these grains and the measured height variation in the range of the film thickness indicate an island film little above the percolation threshold where coalescence just has started. Strong depolarization and enhanced relaxation due to electron-surface scattering are a consequence of such a topography. In contrast, the surface of the Cu film on Si only shows a smooth variation of height with height differences below 1 nm at typical lateral distances of about 10–20 nm. This smoothness aligns with the found $\omega_P^2 \text{ film} / \omega_P^2 \text{ bulk}$ values. The observation of grain boundaries is beyond the resolution of this microscopy experiment.

Summarizing our studies of film morphology, we believe in having prepared conducting films with surfaces of different mesoscopic roughness as sketched in Fig. 1. This is based on our analysis of ir spectroscopic results and supported by our AFM results. From the literature a strong $3d$ -island growth mode (Vollmer-Weber growth) is known for a broad series of metals on ionic crystal surfaces.^{50–52} Generally, the much higher surface free energy of metals compared to insulating compounds is the main reason for this kind of growth. For Cu/Si(111)7×7, the literature reports on RHEED oscillations for growth at ~ 120 K and $d > 1$ nm.^{47,48} Such oscillations indicate a layer-by-layer growth on mesoscopically smooth surfaces.

In this section we estimated filling factors for the prepared films ($F \approx 0.6$ for Cu/KBr and $F \approx 1$ for Cu/Si). This estimation is based on our ir spectroscopic results rather than the AFM results as, e.g., fine trenches or small holes in the film are masked by the finite size and curvature of the tip. These values will be used for the following quantitative discussion of adsorbate effects.

B. Adsorbate exposure

Concerning molecular adsorption, the surfaces of the Cu films on KBr(001) and on Si(111) are both the results of growth at ~ 100 K. At this temperature, RHEED oscillations are observed for Cu/Si(111)^{47,48} and for Cu homoepitaxy,^{53,54} but they are damped out after few monolayers. Hence, for the films on the various substrates the same microscopic (atomic scale) surface roughness is expected and similar adsorbate sticking probabilities and adsorption kinetics may be assumed.

From the very beginning of adsorbate exposure we observed a change in the ir-broadband transmission of the metal thin films on either of the substrates. We find that the ACBT due to CO adsorption saturates at about 2.5 L for Cu/Si and at about 8 L for Cu/KBr. For an analysis of the influence of mesoscopic morphology, we choose exposures above those saturation values [see Fig. 6(a)], i.e., we discuss spectra which represent CO saturation on defect-rich surfaces of Cu at 100 K. For C₂H₄ exposure we find a faster change in ir properties within roughly the first 5 L and further a more gradual change. Up to an exposure of 18 L the films on KBr and on Si did not show a saturation of ACBT. In this case, we decided to compare spectra which were recorded at about the same exposure to C₂H₄ [see Fig. 6(b)].

The spectral shape of the ACBT is different for different adsorbate molecules,²⁰ but also, it is different for the Cu

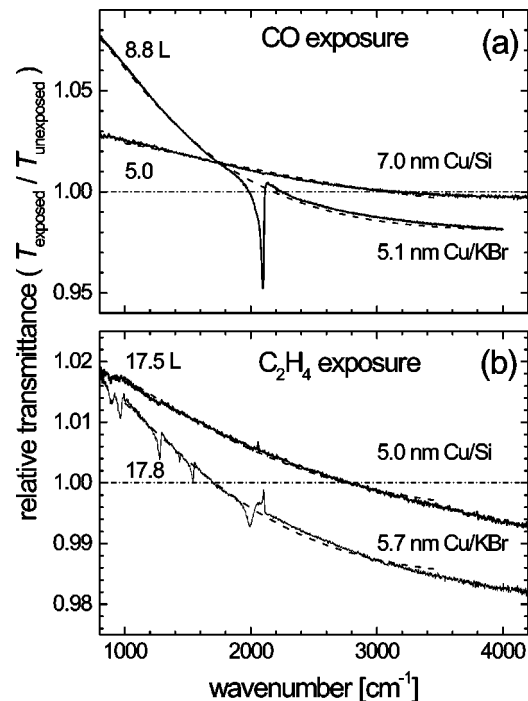


FIG. 6. Spectra of adsorbate-induced change in broadband transmission (ACBT): (a) 5 nm Cu/KBr(001) and 7 nm Cu/Si(111) exposed to CO; (b) 5 nm Cu on KBr(001) and 5 nm Cu on Si(111) exposed to C₂H₄. Solid lines, from experiment; dashed lines, calculated with the values given in Table I. The exposures are indicated by the labels. For the films on KBr the spectra also show absorption lines from adsorbate vibrations. For C₂H₄/Cu/KBr the structure at ~ 2100 cm⁻¹ is due to CO adsorption from the residual gas ($p_{\text{CO}} \leq 10^{-10}$ mbar) prior to C₂H₄ exposure.

films on the different substrates (see Fig. 6) for both CO and C₂H₄. The development of molecular vibration resonances is observed for the two adsorbates on Cu/KBr, but not for Cu/Si. We know that the intensities of these resonances are strongly increased due to SEIRA on rough metal films.^{8,41,49} On Cu films, this enhancement is stronger for CO than for C₂H₄. As a result, CO adsorption from the residual gas (prior to C₂H₄ exposure) leads to SEIRA lines (at ~ 2100 cm⁻¹) of similar strength as the SEIRA lines (between 900 cm⁻¹ and 1600 cm⁻¹) from roughly monolayer coverage of C₂H₄. From the comparison of the CO line in Figs. 6(a) and 6(b), we estimate a precoverage of less than 4% of the surface with CO in the C₂H₄ adsorption experiments. The full spectral description including SEIRA lines is beyond the scope of this paper. A quantitative explanation of these lines was given in recent work.⁷ Here, we analyze the baseline change as described in Sec. II.

Again, excellent spectral accord between experiment and calculation is obtained by fitting the two parameters $\omega_P^2 \text{ film} / \omega_P^2 \text{ bulk}$ and $\omega_{\pi 0}$ (see Fig. 6). We find that adsorbate-induced electronic relaxation (see $\Delta\omega_{\pi 0} \cdot d$ in Table I) and effective charge transfer [see $(\Delta d)_{\text{eff}}$ values in Table I] are both positive for the two films and the two adsorbates. Obviously, the adsorbates act as scatterers for electrons at the Fermi level and they supply charge carriers for transport.²⁰ These properties have contrary effects on the dynamic con-

ductivity with a different balance in the various frequency regions.²¹ For example, they cancel each other at a frequency where the ACBT vanishes (see Fig. 6). From the literature it is known that adsorption of either CO or C₂H₄ increases the dc resistance of smooth Cu films mainly by increasing the relaxation of conduction electrons.^{1,16} This increase is stronger for CO as its lowest unoccupied molecular orbital lies lower than the one from C₂H₄. Charge transfer is expected for various chemisorption systems. While $(\Delta d)_{\text{eff}} < 0$ is expected for strongly electronegative adsorbates, e.g., oxygen,²⁰ the positive $(\Delta d)_{\text{eff}}$ values for CO and C₂H₄ are supported by theoretical work which finds electron donation from the molecules to the metal substrate.⁵⁵

There is a correlation between our results for $\Delta\omega_{\tau} \cdot d$ and $(\Delta d)_{\text{eff}}$ and the morphology of the investigated films. We observed stronger changes for the rough films and smaller changes for the smooth films. But also, the increase due to roughness is only weak for $\Delta\omega_{\tau} \cdot d$ (by a factor of 1.3 for CO and by a factor of 2.2 for C₂H₄), but strong for $(\Delta d)_{\text{eff}}$ (by a factor of 3 for CO and by a factor of 7 for C₂H₄). In the following we analyze this roughness-induced enhancement and its different strength for both these adsorbate effects.

According to the study in Sec. II, our analysis of spectra should yield the genuine values for the relaxation experienced by the charge carriers in either the smooth or the rough films. This means, the factors 1.3 and 2.2 reflect the true increase in charge carrier relaxation which is possibly due to the larger total surface of Cu on KBr compared to Cu on Si. Playing only with surface geometries and assuming island-aspect ratio (height divided by half of the diameter) up to unity, we find for islandlike films a surface area which is typically below a factor of 2 larger than for a smooth film, and even for islands with sharp and fine trenches in between⁵⁶ this factor is below 3. Hence, the enhancement of relaxation can be understood on the basis of the increased surface area.

The roughness-induced strong increase of $(\Delta d)_{\text{eff}}$ cannot be understood purely on the basis of increased surface area. Also, it is certainly not due to a different adsorbate-metal bonding as we know from various ir reflection studies at oblique incidence of adsorbate vibrational frequencies on rough and on smooth films which both were prepared at the same temperature.⁵⁷ We also exclude the background polarizability of the adsorbed molecules as an origin of large $(\Delta d)_{\text{eff}}$ values for inhomogeneous films because this polarizability changes the spectra only for $\omega > \omega_{\text{max}}$, as shown in Sec. II (see Fig. 2). However, our analysis in Sec. II suggests that the spectral fit gives an $(\Delta d)_{\text{eff}}$ which is enhanced with respect to the true charge transfer Δd due to the optical properties of an inhomogeneous metal film. From $\omega_p^2 \text{film} / \omega_p^2 \text{bulk} = 2F - 1$ [see Eq. (12)] we obtain $F \approx 1$ and $S \approx 1$ for the smooth films on Si, but $F \approx 0.6$ and $S \approx 5$ for the rough films on KBr (see Table I). According to this the $(\Delta d)_{\text{eff}}$ values for the rough films are about 5 times larger than Δd , the real amount of charge transfer.

We calculated values for Δd using Eq. (15) and values for $(\Delta d)_{\text{eff}}$ and S from Table I. We get similar values for both smooth and rough films. Taking into account the error in $(\Delta d)_{\text{eff}}$ and the uncertainties in the determination of S , and

keeping in mind that the total surface area of the rough films is by a factor of about 2 larger than for the smooth films, the conclusion is that charge transfer per adsorbate molecule is not measurably influenced by an islandlike morphology, as expected. Rather it is the effective change of dielectric properties which is enhanced by an inhomogeneous morphology.

Note, this conclusion is not restricted to the ir range of frequencies. There is no lower frequency limit for the applicability of the sensitivity S . Hence, our conclusion would also hold for static resistivity measurements. We also want to point out that the enhancement of charge transfer effects is for films already beyond the percolation threshold and, in addition, it is not limited to film thicknesses below the mean free path of the charge carriers. Enhancement effects must be expected for the dielectric response of the free charge carriers in a near-surface region with a thickness in the range of the roughness amplitude. Surface resistivity effects (due to adsorbate induced relaxation) are not enhanced by depolarization.

Let us return to the factor C^* [see Eq. (2)] and its experimental determination according to Eq. (3). The insensitivity of ΔR_p to charge transfer should also hold for metals (or metal films) with an inhomogeneous or granular surface region. This can be seen following Persson's application of the Feibelman d -parameter formalism.⁹ Charge transfer should not influence the imaginary part of d_{\parallel} . As a consequence, for inhomogeneous films with $S > 1$ (at least in the surface region) the experimental results for the factor C^* should deviate from the ideal value [see Eq. (2)] if charge transfer is present. The interpretation of experimental C^* values may lead to unphysical results for $\Delta n/n$, as it has been stated in the literature.¹ Hence, for a quantitative analysis of adsorbate effects in free-electron experiments, ranging from dc resistivity measurement to probing millimeter wave or infrared properties, it is essential to consider the real film microstructure.

Finally, we want to emphasize that our conclusions are based on the quantitative description of optical spectra from inhomogeneous metal thin films. This quantitative description gets by with the minimum number of free parameters. We successfully described the frequency dependent interplay of resistivity effects and chemical effects induced by adsorbates. Nevertheless, the influence of quantum size effects and of nanoscale roughness on adsorbate-induced relaxation and adsorbate-induced charge transfer, e.g., at tunneling sites⁵⁸ were not investigated. However, they may be important for future studies of adsorbate-induced properties of metal nanostructures.

V. SUMMARY

We prepared and studied thin films of copper on Si(111) and on KBr(001). Infrared transmission spectra, measured during growth of the films, and *ex-situ* atomic force microscopy find a granular morphology on KBr and smooth films on Si. We exposed the films to CO and to C₂H₄ and measured their ir transmission during exposure. The transmittance changes were dependent on both the respective adsorbate species and the thin-film morphology. We analyzed this

optical effect by applying a Drude-type model description and determined the adsorbate-induced changes in the charge carrier relaxation and in the thin-film plasma frequency. For the granular morphologies the changes were enhanced compared to the results from the smooth films and this enhancement was stronger for the plasma frequency change compared to the relaxation rate change. We understand this finding on the basis of a model analysis of optical properties of inhomogeneous metal thin films. In a Drude-type analysis of optical spectra the adsorbate effect on the charge carrier relaxation appears unmodified but the effect related to microscopic adsorbate-induced charge transfer is strongly amplified by mesoscopic roughness. According to this, for the investigated rough Cu films the effective adsorbate-induced change in the number of free charge carriers, as deduced from plasma frequencies, is expected to be stronger than can be explained with the increased surface area for adsorption. The latter only explains the weaker roughness effect on the adsorbate-induced charge carrier relaxation.

Our conclusion is that in both static and dynamic conductivity experiments with adsorbates on conductive but inhomogeneous metal thin films the charge-transfer effects are enhanced due to depolarization. In the past, this enhancement has led to conclusions of incomprehensibly large charge transfer effects, which now can be understood. We propose broadband ir spectroscopy of well-defined metal nanostructures and metal nanowires for further investigation of adsorbate effects involved with conduction electrons and quantum confinement.

ACKNOWLEDGMENTS

The authors are grateful to R. G. Tobin for stimulating this work, and to B.N.J. Persson, A. Otto, and F. Forstmann for fruitful and interesting discussions. We thankfully acknowledge financial support by the Deutsche Forschungsgemeinschaft (DFG).

-
- ¹R. G. Tobin, Surf. Sci. **502–503**, 374 (2002).
²M. Hein, P. Dumas, A. Otto, and G. P. Williams, Surf. Sci. **419**, 308 (1999).
³P. Wißmann, in *Surface Physics*, edited by G. Höhler, Springer tracts in Modern Physics, Vol. 77 (Springer, New York, 1975).
⁴G. A. Fried, Y. Zhang, and P. W. Bohn, Thin Solid Films **401**, 171 (2001).
⁵T. Brandt, W. Hoheisel, A. Iline, F. Stiez, and F. Träger, Appl. Phys. B: Lasers Opt. **65**, 793 (1997).
⁶P. Wißmann, in *Handbook of Optical Properties*, edited by R. E. Hummel and P. Wilmann (CRC, New York, 1997), Vol. II.
⁷A. Priebe, M. Sinther, G. Fahsold, and A. Pucci, J. Chem. Phys. **119**, 4887 (2003).
⁸A. Priebe, G. Fahsold, and A. Pucci, Surf. Sci. **482–485**, 90 (2001).
⁹B. N. J. Persson, Phys. Rev. B **44**, 3277 (1991).
¹⁰B. N. J. Persson, Surf. Sci. **269–270**, 103 (1992).
¹¹B. N. J. Persson and A. I. Volokitin, Surf. Sci. **310**, 314 (1994).
¹²M. Hein and D. Schuhmacher, J. Phys. D **28**, 1937 (1995).
¹³C.-L. Hsu, E. F. Mc Cullen, and R. G. Tobin, Chem. Phys. Lett. **316**, 336 (2000).
¹⁴D. E. Kuhl, K. C. Lin, C. Chung, J. S. Luo, H. Wang, and R. G. Tobin, Chem. Phys. **205**, 1 (1996).
¹⁵K. C. Lin, R. G. Tobin, and P. Dumas, Phys. Rev. B **49**, 17 273 (1994).
¹⁶M. Hein, P. Dumas, A. Otto, and G. P. Williams, Surf. Sci. **465**, 249 (2000).
¹⁷P. Dumas, M. Hein, A. Otto, B. N. J. Persson, P. Rudolf, R. Raval, and G. P. Williams, Surf. Sci. **433–435**, 797 (1999).
¹⁸Actually, R. G. Tobin investigated the value of $\omega_p^2 \epsilon_0 / (cC^*)$. Small corrections to his numeric results are necessary if more details of the angular dependence of ΔR are taken into account; see Eq. (3) and Ref. 2.
¹⁹E. T. Krastev, D. E. Kuhl, and R. G. Tobin, Surf. Sci. **387**, L1051 (1997).
²⁰G. Fahsold, M. Sinther, A. Priebe, S. Diez, and A. Pucci, Phys. Rev. B **65**, 235408 (2002).
²¹G. Fahsold, A. Bartel, O. Krauth, N. Magg, and A. Pucci, Phys. Rev. B **61**, 14 108 (2000).
²²Circular frequencies and relaxation rates will be given in wave number units “cm⁻¹.”
²³D. A. Papaconstantopoulos, *Handbook of the Band Structure of Elemental Solids* (Plenum, New York and London, 1986).
²⁴F. Forstmann and R. R. Gerhardts, *Metal Optics Near the Plasma Frequency*, Springer Tracts in Modern Physics, Vol. 109 (Springer, Berlin, 1986).
²⁵M. A. Ordal, R. J. Bell, R. W. Alexander, Jr., L. L. Long, and M. R. Querry, Appl. Opt. **24**, 4493 (1985).
²⁶D. Bergmann, Phys. Rep. **43**, 377 (1978).
²⁷J. C. Maxwell-Garnett, Philos. Trans. R. Soc. London **203**, 385 (1904); **205**, 237 (1906).
²⁸D. A. G. Bruggemann, Ann. Phys. (Leipzig) **24**, 636 (1935).
²⁹A. Bittar, S. Berthier, and J. Lafait, J. Phys. (Paris) **45**, 623 (1984).
³⁰D. A. Aspnes, Thin Solid Films **89**, 249 (1982).
³¹M. M. Dvoynenko, A. V. Goncharenko, V. R. Romaniuk, and E. F. Venger, Physica B **299**, 88 (2001).
³²B. N. J. Persson and J. E. Demuth, Phys. Rev. B **31**, 1856 (1985).
³³X. Zhang and D. Stroud, Phys. Rev. B **52**, 2131 (1995).
³⁴D. Stauffer and A. Aharony, *Introduction to Percolation Theory* (Taylor and Francis, London, 1992).
³⁵S. Berthier and K. Driss-Khodja, Opt. Commun. **70**, 29 (1989).
³⁶W. Theiss, software SCOUT 2 (M.Theiss Hard- and Software, Aachen, Germany, 2000), www.mtheiss.com.
³⁷G. S. Higashi, Y. J. Chabal, G. W. Trucks, and K. Raghavachari, Appl. Phys. Lett. **56**, 656 (1990).
³⁸C.-W. Hu, H. Hibino, T. Ogino, and I. S. T. Tsong, Surf. Sci. **487**, 191 (2001).
³⁹R. A. Lukaszew, Y. Sheng, C. Uher, and R. Clarke, Appl. Phys. Lett. **76**, 724 (2000).
⁴⁰G. Fahsold, A. Bartel, O. Krauth, and A. Lehmann, Surf. Sci. **433–435**, 162 (1999).

- ⁴¹M. Sinther, A. Pucci, A. Otto, A. Priebe, S. Diez, and G. Fahsold (unpublished).
- ⁴²N. W. Ashcroft and N. D. Mermin, *Solid State Physics* (Holt-Saunders International Editions, New York, 1976).
- ⁴³E. H. Sondheimer, *Adv. Phys.* **1**, 1 (1952).
- ⁴⁴G. Fahsold and A. Pucci, in *Advances in Solid State Physics* (Springer, Berlin, 2003), Vol. 43, p. 833.
- ⁴⁵E. F. Mc Cullen, Ching-Ling Hsu, and R. G. Tobin, *Surf. Sci.* **481**, 198 (2001).
- ⁴⁶W. Steinhögl, G. Schindler, G. Steinlesberger, and M. Engelhardt, *Phys. Rev. B* **66**, 075414 (2003).
- ⁴⁷Z. H. Zhang, S. Hasegawa, and S. Ino, *Surf. Sci.* **415**, 363 (1998).
- ⁴⁸T. I. M. Bootsma and T. Hibma, *Surf. Sci.* **331–333**, 636 (1995).
- ⁴⁹O. Krauth, G. Fahsold, N. Magg, and A. Pucci, *J. Chem. Phys.* **113**, 6330 (2000).
- ⁵⁰J. B. Zhou and T. Gustafsson, *Surf. Sci.* **375**, 221 (1997).
- ⁵¹G. Fahsold, A. Pucci, and K.-H. Rieder, *Phys. Rev. B* **61**, 8475 (2000).
- ⁵²M. Bäumer, M. Frank, M. Heemeier, R. Kühnemuth, S. Stempel, and H.-J. Freund, *Surf. Sci.* **454–456**, 957 (2000).
- ⁵³R. Kunkel, B. Poelsema, L. K. Verheij, and G. Comsa, *Phys. Rev. Lett.* **65**, 733 (1990).
- ⁵⁴W. Wulfhekel, N. N. Lipkin, J. Kliewer, G. Rosenfeld, L. C. Jorritsma, B. Poelsema, and G. Comsa, *Surf. Sci.* **348**, 227 (1996).
- ⁵⁵A. Zangwill, *Physics at Surfaces* (Cambridge University Press, Cambridge, 1988).
- ⁵⁶M. Kalff, P. Šmilauer, G. Comsa, and T. Michely, *Surf. Sci. Lett.* **426**, L447 (1999).
- ⁵⁷M. Sinther, thesis, Universität Heidelberg, 2002.
- ⁵⁸C. Holzapfel, F. Stubenrauch, D. Schumacher, and A. Otto, *Thin Solid Films* **188**, 7 (1990).